Biochimica et Biophysica Acta 1821 (2012) 1167–1176

Contents lists available at SciVerse ScienceDirect

Biochimica et Biophysica Acta

journal homepage: www.elsevier.com/locate/bbalip

Modulation of excitability, membrane currents and survival of cardiac myocytes by N-acylethanolamines

Oleg I. Voitychuk [a,c], Valentyna S. Asmolkova [b], Nadiya M. Gula [b], Ganna V. Sotkis [a,c], Sehamuddin Galadari [d], Frank C. Howarth [e], Murat Oz [f], Yaroslav M. Shuba [a,c,*]

[a] Bogomoletz Institute of Physiology and International Center of Molecular Physiology of the National Academy of Sciences of Ukraine, Kyiv, Ukraine
[b] Palladin Institute of Biochemistry of the National Academy of Sciences of Ukraine, Kyiv, Ukraine
[c] State Key Laboratory of Molecular and Cellular Physiology, Kyiv, Ukraine
[d] Department of Biochemistry, Faculty of Medicine and Health Sciences, UAE University, Al Ain, United Arab Emirates
[e] Department of Physiology, Faculty of Medicine and Health Sciences, UAE University, Al Ain, United Arab Emirates
[f] Department of Pharmacology, Faculty of Medicine and Health Sciences, UAE University, Al Ain, United Arab Emirates

ARTICLE INFO

Article history:
Received 30 December 2011
Received in revised form 17 April 2012
Accepted 11 May 2012
Available online 18 May 2012

Keywords:
Cardiac myocyte
Endocannabinoid
Excitability
Ion channel

ABSTRACT

N-Acylethanolamines (NAE) are endogenously produced lipids playing important roles in a diverse range of physiological and pathological conditions. In the present study, using whole-cell patch clamp technique, we have for the first time investigated the effects of the most abundantly produced NAEs, N-stearoylethanolamine (SEA) and N-oleoylethanolamine (OEA), on electric excitability and membrane currents in cardiomyocytes isolated from endocardial, epicardial, and atrial regions of neonatal rat heart. SEA and OEA (1–10 μM) attenuated electrical activity of the myocytes from all regions of the cardiac muscle by hyperpolarizing resting potential, reducing amplitude, and shortening the duration of the action potential. However, the magnitudes of these effects varied significantly depending on the type of cardiac myocyte (i.e., endocardial, epicardial, atrial) with OEA being generally more potent. OEA and to a lesser extent SEA suppressed in a concentration-dependent manner currents through voltage-gated Na^+ (VGSC) and L-type Ca^{2+} (VGCC) channels, but induced variable cardiac myocyte type-dependent effects on background K^+ and Cl^- conductance. The mechanisms of inhibitory action of OEA on cardiac VGSCs and VGCCs involved influence on channels' activation/inactivation gating and partial blockade of ion permeation. OEA also enhanced the viability of cardiac myocytes by reducing necrosis without a significant effect on apoptosis. We conclude that SEA and OEA attenuate the excitability of cardiac myocytes mainly through inhibition of VGSCs and VGCC-mediated Ca^{2+} entry. Since NAEs are known to increase during tissue ischemia and infarction, these effects of NAEs may mediate some of their cardioprotective actions during these pathological conditions.

1. Introduction

N-Acylethanolamines (NAEs) are produced endogenously from glycerophospholipids. They comprise a diverse family of signaling lipids and are found ubiquitously in a broad spectrum of species ranging from mammalian and invertebrates to plants and microorganisms (for reviews see [1–3]). In recent decades research on the biological actions of NAEs has received much attention mainly due to the ability of polyunsaturated NAEs such as N-arachidonoylethanolamine (AEA), also known as anandamide, to bind to and activate cannabinoid (CB) receptors (for reviews see [4,5]).

NAEs content in various mammalian tissues ranges from about 0.1 to 20 nmol/g [2], but the levels of NAEs and their precursors N-acylphosphatidylethanolamines (NAPEs) increase quite dramatically under various types of cell stress [1]. Normal heart does not contain perceptible amounts of NAEs [6,7], however, earlier studies in cardiac muscle have revealed considerable elevation of NAEs content under hypoxic conditions when extensive membrane degradation occurs, e.g., in myocardial infarction [1,6,8,9]. These findings are not surprising since mammalian cardiac muscle exhibits high metabolic activity, which is dependent predominantly on fatty acids for energy, and requires a high amount of oxygen for normal function.

Accumulation of NAEs was first observed in experimental myocardial infarction induced by ligation of coronary arteries in canine heart [6,8]. It was demonstrated that NAE content increases up to 500 nmol/g (approximately 500 μM) in infarcted areas of canine heart during ischemia [6]. Importantly, these high NAE levels were detected only in damaged areas of the heart and were not present at all in normal areas of the same heart [6,8]. Thus, the hypoxic or anoxic conditions are known

Abbreviations: AP, action potential; APD, action potential duration; NAE, N-acylethanolamines; SEA, N-stearoylethanolamine; OEA, N-oleoylethanolamine; PM, plasma membrane; VGCC, voltage-gated Ca^{2+} channel; VGSC, voltage-gated Na^+ channel

* Corresponding author at: Bogomoletz Institute of Physiology NASU, Bogomoletz Str., 4, Kyiv, 01024, Ukraine.
E-mail address: yshuba@biph.kiev.ua (Y.M. Shuba).

1388-1981/$ – see front matter © 2012 Elsevier B.V. All rights reserved.
doi:10.1016/j.bbalip.2012.05.003

to have very rapid and drastic consequences with respect to performance, ultrastructure and metabolism in cardiac tissue.

The NAEs consist almost exclusively of palmitic, stearic, oleic, and linoleic acids [1] with N-stearoylethanolamine (SEA, 18:0 NAE) and N-oleoylethanolamine (OEA, 18:1 NAE) being major saturated and monounsaturated NAE species, respectively. Although, biochemical aspects of NAE synthesis have been studied relatively well, functional importance and cellular targets for these NAEs are currently unknown. In this study we have investigated the effects of SEA and OEA, major NAEs elevated during ischemia [1] on electrical excitability and underlying membrane currents in rat neonatal cardiac myocytes. Our data show that both SEA and OEA exert attenuating effects on cardiac excitability mainly due to inhibition of the inward voltage-gated sodium and calcium currents and in part potentiation of the background potassium and/or chloride currents, which may underlie their cardioprotective properties. Preliminary results of the study have been presented earlier [10,11].

2. Materials and methods

2.1. Cell culture

Isolation and culturing of neonatal rat cardiac myocytes were performed under aseptic conditions according to the general procedure described elsewhere [12]. Briefly, 3-day-old pups were decapitated, their hearts quickly removed and placed into ice-cold Ca^{2+}-free physiological saline (PhS, in mM): 144 NaCl, 4 KCl, 1 $MgSO_4$, 1.2 KH_2PO_4, 0.43 Na_2HPO_4, 5 sodium pyruvate, 10 HEPES, 10 glucose, and pH 7.35 (adjusted with NaOH). The hearts were cut into small pieces (~1 mm^3), which were transferred to Ca^{2+}-free PhS bubbled with carbogen (gas mixture of 95% O_2 and 5% CO_2) at room temperature. Enzymatic digestion was performed in the same solution supplemented with 0.46 mg/ml collagenase (Type IA, Sigma-Aldrich) at 37 °C for 30 min with slight agitation and bubbling with carbogen. Then the tissue was transferred into enzyme-free solution where it was dispersed by pipetting. The suspension was centrifuged at 3000 rpm, the supernatant was removed and the pellet was resuspended in the PhS with Ca^{2+} concentration increased to 0.2 mM. The Ca^{2+} concentration in this solution was then gradually increased to 1.5 mM over 1 h. After another centrifugation at 3000 rpm the cell pellet was resuspended in DMEM culture medium supplemented with 10% of fetal calf serum (Gibco–Invitrogen). Cells were plated onto gelatin-coated glass cover slips at approximate density of 100,000 cm^{-2} and placed in a petri dish filled with culture medium. Cells were maintained in the incubator in a 5% CO_2 + 95% O_2 atmosphere at 37 °C for 1–3 days. The culture medium was changed every 24 h.

2.2. Electrophysiology, solutions and $[Ca^{2+}]_i$ measurements

Whole-cell patch-clamp experiments in cultured cardiac myocytes were performed using PC-ONE (Dagan Corp, Minneapolis, MN) amplifier and pClamp 8.0 software (Molecular Devices, Union City, CA) for data acquisition and analysis. Patch pipettes for the whole-cell recordings were fabricated from borosilicate glass capillaries (World Precision Instr., Inc., Sarasota, FL) on a horizontal puller (Sutter Instruments Co., Novato, CA) and had resistances of 2–3 MΩ when filled with intracellular solutions.

Basic extracellular solutions used for electrophysiological recordings contained (in mM): 144 NaCl, 5.4 KCl, 1.8 $CaCl_2$, 1.2 $MgCl_2$, 1 NaH_2PO_4, 10 HEPES, 10 glucose, and pH 7.4 (adjusted with NaOH). Recording patch pipettes were filled with intracellular solution containing (in mM): 10 KCl, 10 KOH, 105 K-aspartate, 15 NaCl, 1 $MgCl_2$, 10 HEPES, 4 Mg-ATP, 5 sucrose, and pH 7.2 (adjusted with HCl). Changes of external solutions and application of drugs were performed using a multi-barrel puffing micropipette with a common outflow positioned in close proximity to the cell under investigation. During the experiment, the cell was continuously superfused with the solution via a puffing pipette to reduce possible artifacts related to the switch from a static to a moving solution and vice versa. Complete external solution exchange was achieved in <1 s. All chemicals except for SEA and OEA (synthesized in the Institute of Biological Chemistry NASU, Kyiv, Ukraine) were obtained from Sigma-Aldrich. SEA and OEA were dissolved in DMSO as 40 or 200 mM stocks and added to the basic extracellular solution in the appropriate amount to achieve the desired final concentration. The concentration of DMSO in the bathing solutions did not exceed 0.05%. Control experiments with applications of DMSO alone at concentrations as high as 0.1% showed no effect on the parameters and events reported in this study.

Electrophysiological data were analyzed using pClamp 8.0 (Molecular Devices, Union City, CA), Origin 7.0 (OriginLab Corp., Northampton, MA) and Matlab (MathWorks Corp., Natick, MA) software. Action potential duration (APD) was measured at different levels of repolarization, 20%, 60% or 90%, from AP amplitude. When constructing current–voltage (I–V) and dose–response relationships the amplitudes of the currents were normalized to the cell membrane capacitance to provide current densities (nA/pF). For obtaining concentration–response relationship, current densities in various myocytes under the action of each SEA or OEA concentration were averaged and fitted to the Hill equation. Cardiac myocytes were classified on types solely based on the shape of the action potential. Therefore, such classification was possible only in current-clamp, but not in voltage-clamp experiments. Endocardial cells were further separated into type 1 and type 2 cells based on the modality and reversibility of SEA actions on the parameters of the AP of corresponding shape. Cultured cardiac myocytes lose their morphology, therefore, no other functional and/or morphological evidence for such separation were available.

Intracellular Ca^{2+} ($[Ca^{2+}]_i$) transients were measured in Fluo-4AM-loaded rat neonatal cardiac myocytes using inverted Olympus IX71 fluorescence microscope equipped with CFW-1312C digital camera (Scion Corp., Frederick, ME) operating at a frame rate 7.5/s. Signal intensity was averaged for the myocyte's area and normalized to the baseline intensity before any intervention was administered.

2.3. Cell viability

The number of live, necrotic and apoptotic cells was determined by staining with bisbenzimide (Hoechst 33342) and propidium iodide (both at the same concentration of 8.75 μM) with subsequent examination by fluorescence microscopy. Bisbenzimide penetrates the cell via intact plasma membrane (PM) and stains nuclear chromatin enabling visualization of the apoptotic cells characterized by fragmented pyknotic nuclei. On the other hand, propidium iodide cannot pass through the intact PM and, thus, stains only nuclei of the necrotic cells, which have damaged PM. Five-hundred cells were counted in each assay.

2.4. Data analysis

Each experiment was performed on several myocytes from different cultures. Since the results of identical experiments from different cultures were qualitatively similar, the data were pooled for statistical purposes with "n" denoting the total number of cells tested for a particular data point. The results of the experiments were expressed as mean ± standard error of the mean (s.e.m.). Statistical analysis was performed using the Student's *t*-test and ANOVA tests followed by Tukey–Kramer post-tests. On all graphs (*) and (**) denote statistical significance with $P<0.05$ and $P<0.02$, respectively, between specified values, or if not specified to the respective control.

3. Results

3.1. The effects of SEA and OEA on electrical activity of cultured rat neonatal cardiomyocytes

Generation of the cardiac action potential involves concerted activation of many ion channels. NAEs are potentially capable of influencing several of these channels either directly or indirectly thereby affecting

cardiac excitability. Thus, examining the effects of NAEs on general excitability of native cardiac myocytes: their resting potential (V_{rest}) and parameters of the action potential (AP) will provide a clue as to which channels are affected. These experiments were carried out by exposing patch-clamped cultured neonatal rat cardiomyocytes to the NAEs (SEA or OEA) while continuously monitoring their V_{rest} and APs in the current-clamp mode. The generation of APs was evoked by 400 pA depolarizing current pulses of 3 ms duration applied at a frequency of 0.2 Hz. Since the intracellular pipette solution did not contain Ca^{2+}-chelating agents, the generation of each AP was accompanied by the cardiac myocyte contraction. A typical experimental protocol included: 1) establishment of the whole-cell configuration, 2) 3–5 minute dialysis of the myocyte with pipette solution to allow all changes in V_{rest} and AP related to the replacement of intracellular milieu to occur, 3) recording of the myocyte's baseline electrical activity following stabilization of V_{rest} and AP parameters, 4) exposure of the myocyte to the studied NAE and observation of NAE-evoked changes, and 5) washout of the NAE after these changes reached a steady-state level.

Fig. 1 presents the results of typical experiments on the effects of 1 μM SEA on the AP of cardiac myocytes from various parts of neonatal rat heart, as judged from the initial shape of the AP. In the ventricular endocardial (Fig. 1A, B), epicardial (Fig. 1C) as well as atrial (Fig. 1D) myocytes SEA consistently shortened the AP duration (measured at 60% of repolarization, APD_{60}) by 4–6 ms (Fig. 2A). However, the influence of the compound on V_{rest} appeared to be more heterogeneous. In about 60% of endocardial cells (type 1 cells) SEA depolarized V_{rest} by 3–4 mV, whereas in the remaining ~40% of the cells (type 2 cells) it caused V_{rest} hyperpolarization by 2–3 mV (Figs. 1A, B and 2B). In all ventricular epicardial myocytes SEA produced V_{rest} depolarization (Figs. 1C, 2B) and in all atrial myocytes — hyperpolarization (Figs. 1D, 2B). The absolute values of SEA-evoked V_{rest} depolarization and hyperpolarization were similar in all types of the myocytes constituting on average 2–4 mV (Fig. 2B). Steady-state AP shortening and changes of V_{rest} in response to SEA application occurred quite fast — within 5–10 s, but required much longer time to recover upon SEA washout with variable cell type-dependent degree of reversibility (Fig. 2A, B).

SEA also decreased the amplitude of the AP and its initial rate of rise in all types of cardiac myocytes (Fig. 3A, B). In the atrial and type 2 endocardial cells the decrease of AP amplitude under SEA action was less pronounced than in type 1 endocardial and epicardial cells. In addition, SEA differentially affected the ratio of APD at 20% and 90% levels of repolarization (APD_{20}/APD_{90}), which characterizes alterations of the shape of AP due to possible preferential SEA action on different AP phases. As shown in Fig. 3C, SEA hardly changed APD_{20}/APD_{90} value compared to control in type 1 endocardial cells, but it caused statistically significant decrease of APD_{20}/APD_{90} value in other cell types, indicating that in all but type 1 endocardial cells SEA acts more potently on membrane conductances that contribute to the upstroke and plateau phase of the AP.

SEA-induced shortening of APD in ventricular myocytes was concentration dependent with EC_{50} value of ~1.5 μM, whereas maximal depolarization of the V_{rest} in the type 1 endocardial and epicardial ventricular myocytes already occurred at a SEA concentration of 0.2 μM hardly changing with increase concentrations up to 5.0 μM (data not shown), suggesting that SEA acts on multiple cardiac ion channels with variable sensitivity.

The effects of monounsaturated OEA on cardiac myocytes' excitability were somewhat different from those of SEA. As documented in Figs. 4 and 2C, D, OEA (1 μM) irrespective of the cell type and in contrast to SEA consistently produced AP shortening and hyperpolarizing shift of V_{rest}. In addition, the reversibility of the OEA effects at least in endocardial ventricular myocytes was better compared to SEA: restoration of the AP and especially V_{rest} values was faster and more complete (Figs. 3A, 2C, D).

Similarly to SEA, OEA reversibly decreased amplitude and initial rate of rise of the AP (Fig. 3D, E). OEA also produced a slight decrease of APD_{20}/APD_{90} in endocardial cells, but increased this ratio in epicardial and atrial cells (Fig. 3F), indicating differential cell-specific expression of ion channels that gives shape to AP in various cell types as well as sensitivity of these channels to OEA.

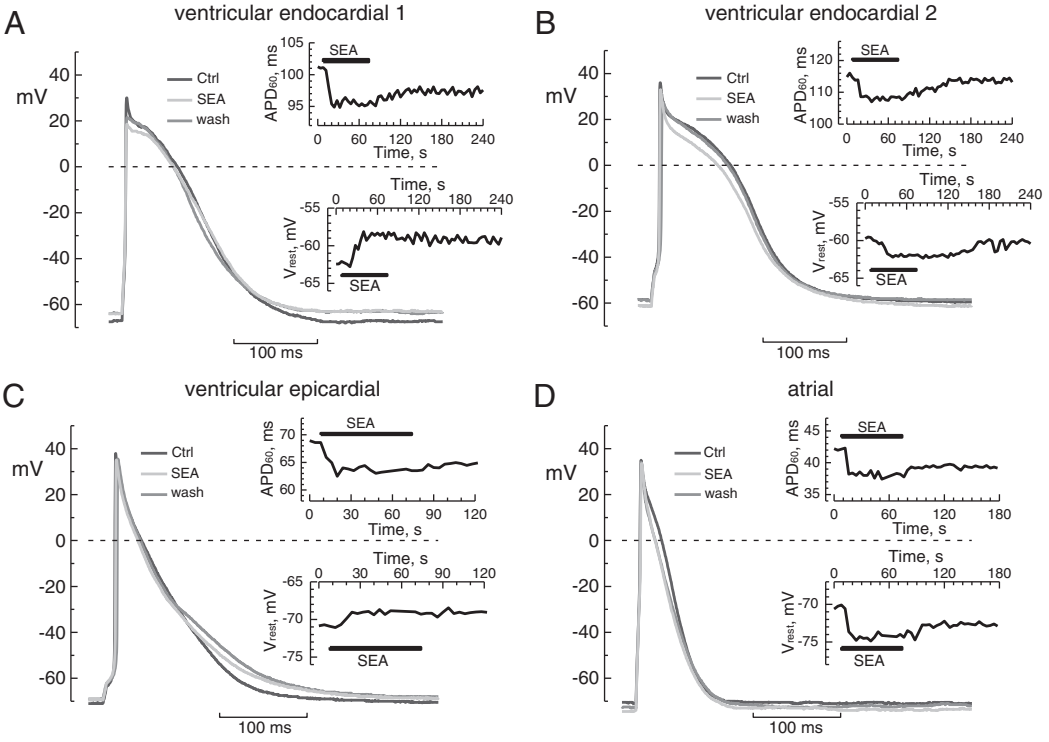

Fig. 1. Effects of SEA on excitability of rat neonatal cultured cardiac myocytes. A–D: Representative recordings of the control action potential (AP, black lines), AP in the presence of 1 μM SEA (light grey lines) and AP after SEA washout (dark grey lines) in the ventricular endocardial type 1 (A), ventricular endocardial type 2 (B), epicardial (C) and atrial (D) cardiac myocytes; the insets on panels A–D show the dynamics of the action potential duration (APD_{60}) and resting potential (V_r) changes in response to SEA application (marked by horizontal bars).

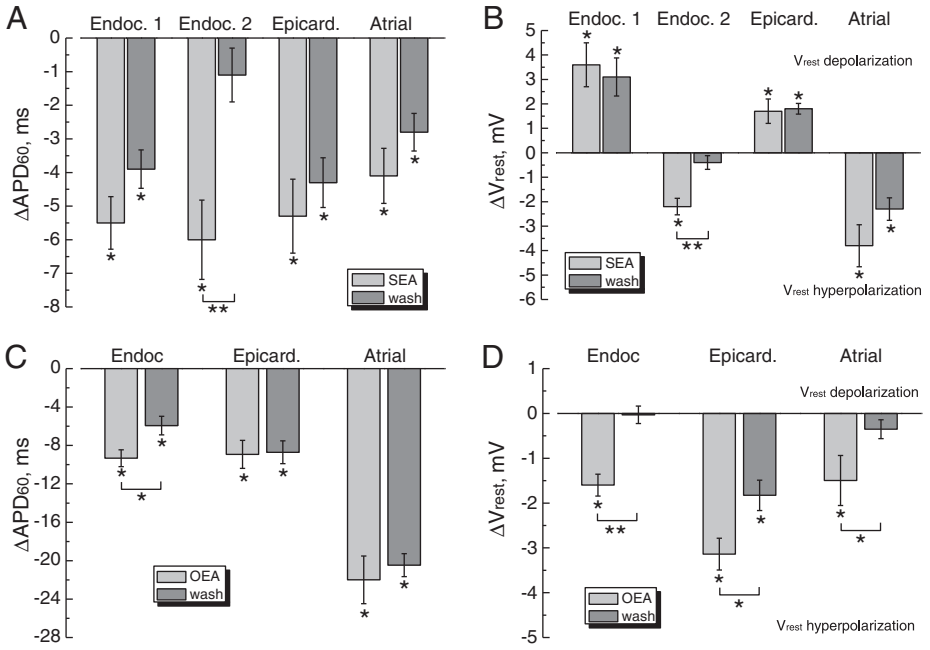

Fig. 2. Quantification of SEA and OEA effects on action potential duration (APD_{60}) and the resting potential (V_{rest}) in different types of rat neonatal cultured cardiac myocytes. A, B: Bar graphs showing changes of APD_{60} (ΔAPD_{60}, A) and V_{rest} (ΔV_{rest}, B) relative to the respective control values in the presence of 1 μM SEA (light grey columns) and following its washout (grey columns); mean ± s.e.m., from 5 to 7 myocytes of each type; asterisks indicate statistically significant difference from "0" (i.e., no change) or between specified values. C, D: same as in A, B, respectively, in the presence of 1 μM OEA and without separation of ventricular endocardial myocytes onto two subtypes.

3.2. The action of SEA and OEA on inward currents of neonatal rat cultured cardiomyocytes

The influence of SEA and OEA on the amplitude and initial rate of rise of the APs indicated that these compounds may affect voltage-activated inward sodium (I_{Na}) and calcium (I_{Ca}) currents of isolated cardiac myocytes. To verify these possibilities, we have conducted a series of experiments under conditions that enable reliable isolation of either I_{Na} or I_{Ca} in voltage-clamp mode.

With 35 mM Na^+ outside and Cs^+ as the major intracellular cation inward I_{Na} in response to incremental step depolarizations (V_m, 10 mV increment) applied from a holding potential $V_h = -90$ mV started to activate at $V_m = -70$ mV, and reached maximal amplitude at $V_m = -20$ mV. At more positive V_m the inward current decreased reversing its direction at an apparent reversal potential (V_{rev}) of around +60 mV due to poor selectivity of voltage-gated sodium channels (VGSC) allowing them to pass Cs^+ in the outward direction (Fig. 5A, B).

Application of SEA even in concentrations as high as 100 μM decreased I_{Na} amplitude at $V_m = -20$ mV at most by 4% (Fig. 5A, B). OEA appeared to be more effective inducing rapid (within <1 min) concentration-dependent inhibition of I_{Na}, which at 100 μM of OEA reached almost 30% (Fig. 5A–C). Fit of experimental data points for concentration-dependency of I_{Na} inhibition by OEA at $V_m = -20$ mV with Hill equation (Fig. 5C) provided values of maximal inhibition at saturating concentration of the compound, $A = 29.9 \pm 0.8\%$, apparent half-maximal inhibitory concentration, $IC_{50} = 8.3 \pm 0.8$ μM, and cooperativity (Hill) coefficient, $p = 1.4 \pm 0.3$.

Comparison of the normalized and then averaged I–V relationships of I_{Na} under control conditions and in the presence of 100 μM of SEA or OEA (Fig. 5B) did not reveal any significant changes of the current's V_{rev}, indicating that these compounds do not alter the selectivity of the underlying VGSCs. Steady-state activation (SSA) curves of I_{Na} before and after the action of SEA or OEA (Fig. 5D) were derived by fitting the respective I–V relationships with the product of Boltzmann and Goldman–Hodgkin–Katz (GHK) equations of which the first one describes voltage-dependence of SSA, and the second one the current through open channels. This allowed one to determine whether or not SEA and OEA influence the parameters of I_{Na} SSA —the voltage of half-maximal activation, $V_{1/2}$, and slope factor, k. It appeared that if for control I_{Na} $V_{1/2} = -34.2$ mV and $k = 8.2$ mV then application of 100 μM of SEA or OEA produced statistically insignificant changes of these parameters in the event of SEA to $V_{1/2} = -36.5$ mV (i.e., hyperpolarizing shift by 2.4 mV) and $k = 8.5$ mV and in the event of OEA to $V_{1/2} = -37.1$ mV (i.e., hyperpolarizing shift by 2.9 mV) and $k = 8.4$ mV (Fig. 5D).

In order to determine whether or not SEA or OAE influences the properties of VGSCs inactivation we compared steady-state inactivation (SSI) dependencies of control I_{Na} and I_{Na} in the presence of each compound. SSI-curves were acquired using a standard voltage protocol consisting of prolonged (400 ms) conditioning pre-pulse to various V_m in the range −100 to +70 mV which was immediately followed by the constant I_{Na}-activating test pulse to $V_m = -20$ mV. SSI-dependency was plotted as normalized amplitude of I_{Na} at $V_m = -20$ mV against the value of conditioning V_m (normalization was performed to the amplitude of I_{Na} at conditioning $V_m = -100$ mV). The fit of the obtained data points using the Boltzmann equation (Fig. 5D) has shown that under control conditions SSI of I_{Na} is characterized by $V_{1/2} = -78.6$ mV and $k = 7.5$ mV, which in the presence of 100 μM of SEA change to $V_{1/2} = -89.3$ mV and $k = 7.4$ mV and in the presence of 100 μM of OEA — to $V_{1/2} = -92.5$ mV and $k = 7.8$ mV. Thus, both NAEs induced sizable hyperpolarizing shifts in the voltage-dependence of SSI of cardiac VGSCs, which for OEA appeared to be more pronounced than for SEA (i.e., −14.0 mV vs. −10.6 mV, respectively).

Comparison of the recordings of the control I_{Na} and I_{Na} in the presence of either SEA or OEA also revealed noticeable acceleration of the current's inactivation kinetics under the action of both NAEs. Quantification of the time constant of I_{Na} inactivation (τ_i, Fig. 5E) by fitting the currents' decay phase with exponential functions has shown that SEA and OEA (both at 100 μM) significantly reduced τ_i in the range of V_m below −30 mV and above +10 mV.

Using the same experimental protocols, the effects of apparently more potent of the two NAEs, OEA, were also investigated on the biophysical properties of high voltage-activated calcium current. I_{Ca} of isolated cardiac myocytes was recorded in the presence of intracellular

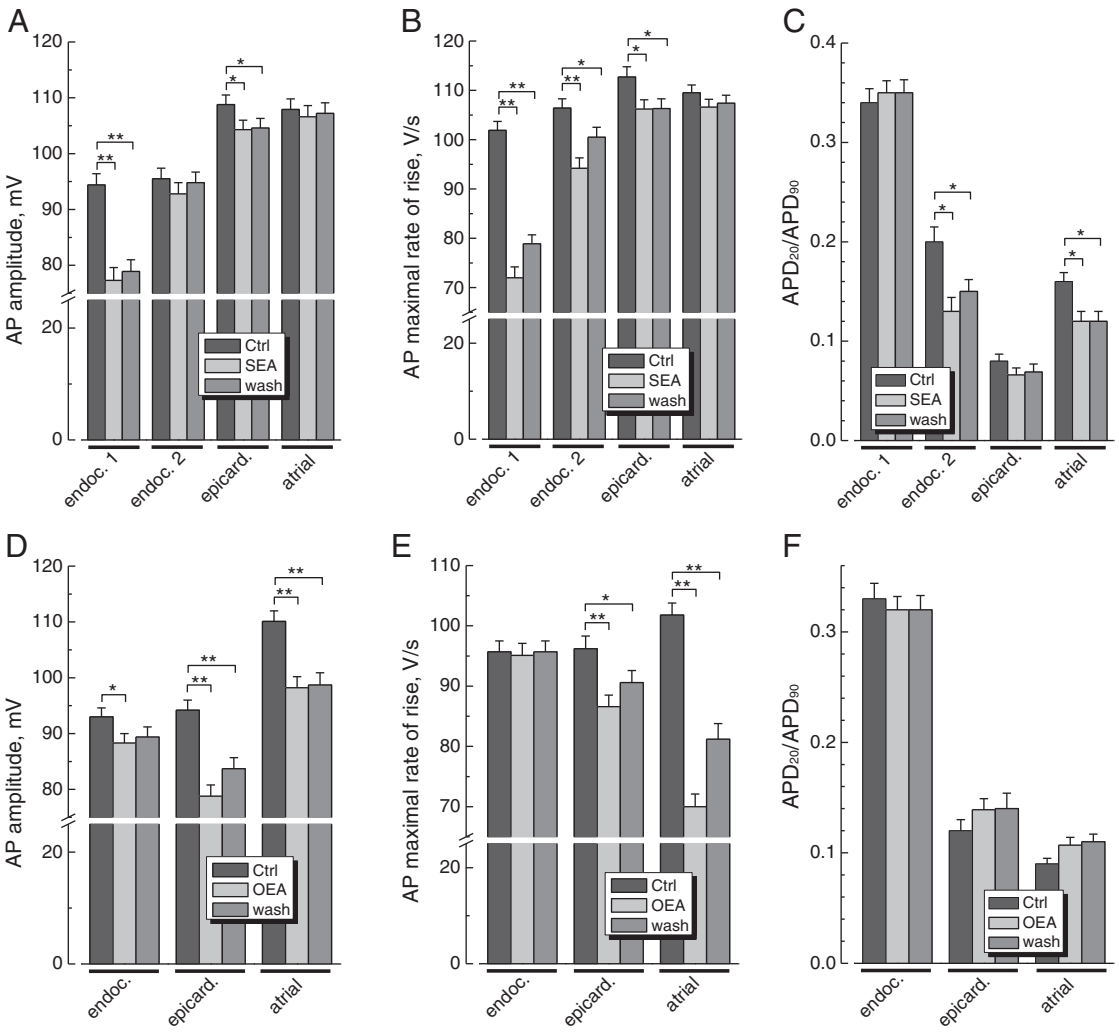

Fig. 3. Effects of SEA and OEA on amplitude and shape of the action potential (AP) in rat neonatal cultured cardiac myocytes. A, B, C: Quantification of the changes of the AP amplitude (A), AP maximal rate of rise (B) and AP shape (C, characterized by the APD_{20}/APD_{90} ratio) in the ventricular endocardial type 1, ventricular endocardial type 2, epicardial and atrial cardiac myocytes in response to 1 μM SEA (light grey columns) and following its washout (grey columns) relative to the control pre-drug values (dark grey columns); mean ± s.e.m., from 5 to 7 myocytes. D, E, F: same as in A, B, C, respectively, but in the presence of 1 μM OAE and without separation of ventricular endocardial myocytes onto two subtypes.

Cs^+ and extracellular TEA^+ to suppress K^+ currents while retaining 20 mM Na^+ in the extracellular saline, since according to our data (not shown) as well as of others [13,14] complete removal of Na^+ results in a notable decrease of I_{Ca} amplitude. Elimination of contaminating sodium current during recording of I_{Ca} was achieved by applying I_{Ca}-activating> voltage step-pulses from relatively depolarized V_h of −50 mV, which produced steady-state I_{Na} inactivation. As evident from original recordings and I–V relationships (Fig. 6A, B), inward I_{Ca} had much slower kinetics in response to step depolarization and activated at more positive potentials than I_{Na}: it started to appear at $V_m = -30$ mV, reached maximum at $V_m = 0$ mV, and decreased at higher voltages approaching zero at about $V_m = +60$ mV (Fig. 6B).

Application of OEA inhibited I_{Ca} in a concentration-dependent manner. Construction of a concentration–response relationship and its fit with Hill equation (Fig. 6C) showed that OEA inhibited I_{Ca} with somewhat lower affinity (i.e., apparent $IC_{50} = 10.2 \pm 0.6$ μM), similar cooperativity (i.e. Hill coefficient $p = 1.36 \pm 0.2$), but two-fold higher efficacy (i.e., maximal block at saturating concentration $A = 72.0 \pm 2.9\%$) compared to I_{Na} (see Fig. 5C for comparison). OEA also produced a depolarizing shift of I_{Ca} SSA by 3.6 mV (i.e., from control value $V_{1/2} = -8.8 \pm 0.2$ mV to $V_{1/2} = -5.2 \pm 0.1$ mV in the presence of OEA) and hyperpolarizing shift of I_{Ca} SSI by 5.2 mV (from control value $V_{1/2} = -15.9 \pm 0.1$ mV to $V_{1/2} = -21.1 \pm 0.1$ mV in the presence of OEA) with little influence on the slopes of respective dependencies ($k = 8.2 \pm 0.2$ mV and $k = -5.9 \pm 0.1$ mV for the control activation and inactivation, respectively, vs. $k = 7.9 \pm 0.1$ mV and $k = -5.1 \pm 0.1$ mV for the OEA-modified activation and inactivation, respectively), which altogether resulted in the notable reduction of I_{Ca} "window current" responsible for the stationary Ca^{2+} entry in the range of membrane potentials from −40 mV to +10 mV (Fig. 6D). Thus, the mechanism of OEA action on cardiac L-type voltage-gated calcium channels (VGCC) most likely involves influence on channel gating that reduces "window current" as well as partial blockade of the ion-conducting pathway that decreases current amplitude.

In spontaneously beating myocytes application of OEA (100 μM) resulted in the pronounced decrease of the amplitude of intracellular Ca^{2+} ($[Ca^{2+}]_i$) transients that accompanied each beat (Fig. 6E) and to the marked attenuation of the beating magnitude, indicating that OEA-mediated inhibition of VGCC may have functional consequences in inducing negative inotropic effect.

3.3. The action of SEA and OEA on the background conductance of neonatal rat cultured cardiomyocytes

The fact that SEA and OEA affected resting membrane potential and shortened AP duration indicated they may influence potassium and/or chloride channels of cardiac myocytes' that contribute to the background conductance and repolarization phase of the AP. To investigate

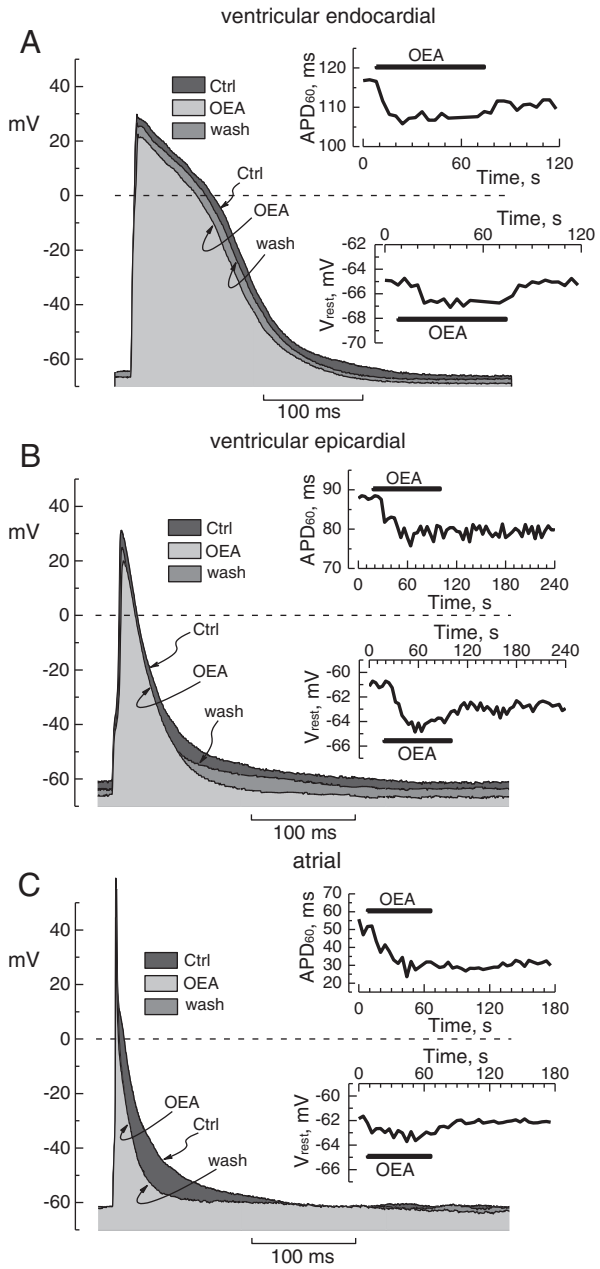

Fig. 4. Effects of OEA on excitability of the rat neonatal cultured cardiac myocytes. A–C: Representative recordings of the control action potential (AP, dark grey fill area under the curve), AP in the presence of 1 μM OEA (light grey fill area under the curve) and AP after OEA washout (grey fill area under the curve) in the ventricular endocardial (A), epicardial (B) and atrial (C) cardiac myocytes; the insets on panels A–C show the dynamics of the action potential duration (APD_{60}) and resting potential (V_r) changes in response to OEA application (marked by horizontal bars).

this, whole-cell patch-clamp experiments were performed in voltage-clamp mode on myocytes bathed in normal Tyrode solution and dialyzed with K^+-based intracellular solution. For myocyte stimulation, a pulse protocol was used that included a voltage-ramp to enable measurements of the current–voltage (I–V) relationship, and the effect of SEA and OEA was examined on the net current activated by such pulses. Potassium and chloride conductances in cardiac myocytes are generated by multiple types of K^+ and Cl^- channels [15,16], however, since we were interested in the overall effect of SEA and OEA on these conductances, no attempt was made to separate the net current on the components passing through different types of K^+- and Cl^--channels.

I–V relationships of the net background current activated by ramp pulses had a reversal potential (V_{rev}) of around −50 mV (Fig. 7A, B), which represented an intermediate value between the K^+ (V_K) and Cl^- (V_{Cl}) equilibrium potentials calculated from the Nernst equation (i.e., $V_K = -79$ mV and $V_{Cl} = -44$ mV under our experimental ionic conditions). Application of SEA had quite variable effects on the current's V_{rev} as well as on its magnitude measured at +100 mV (data not shown), consistent with the myocyte's type-dependent disparity of action of this compound on V_{rest} and APD (see Fig. 3). With OEA the effects were more consistent: 29 cells tested with respect to the action of OEA on their background current could be separated into three groups: the first, also the most numerous group, showed basically no change, the second showed current decrease and the third responded by current enhancement (Fig. 7C). In the latter group of cells increase of the background current was accompanied by a negative shift of the V_{rev} by about 5 mV (Fig. 7B, C), which, given that the shift occurred towards V_K, indicated activation of K^+ component of the background current.

3.4. OEA decreases cadiomyocytes' necrosis

To determine whether attenuating effects of SEA and OEA on cardiac excitability are associated with altered viability of cardiac myocytes we have compared the myocytes' apoptosis and necrosis under control conditions and in the presence of the more potent of the two compounds, OEA. Fig. 8 shows that addition of OEA concentration-dependently enhanced myocytes' viability compared to control, which at 100 μM of OEA reached statistical significance (i.e., 90 ± 2% of surviving cells after 24 h of culturing in the presence of OEA vs. 82 ± 1.5% of surviving cells under control conditions). The enhancement of cells' viability appeared to primarily result from inhibition of necrosis even though cells' apoptosis was insignificantly increased by OEA (Fig. 8). These results suggest that OEA mostly protects cardiac myocytes from the naturally-occurring damage at the level of the cell membrane despite slight stimulation of the intrinsic apoptotic machinery. The protective effects of OEA may at least in part be explained by the inhibition of steady-state Ca^{2+} influx due to reduction of the "window current" through the L-type VGCC (see Fig. 6D).

4. Discussion

In the present study we have demonstrated that SEA and OEA modulate the excitability of cardiomyocytes by influencing resting membrane potential, V_{rest}, and duration and amplitude of the action potential. This, to our knowledge, is the first study providing systematic examination of the effects of the most abundant NAEs, saturated SEA and monounsaturated OEA which are produced during ischemia, on electrical excitability and underlying membrane currents of cardiac myocytes.

SEA and OEA produced complex, cardiac myocyte type-dependent alterations in the V_{rest}, APD and AP amplitude which varied quantitatively among different types of cardiomyocytes, but could be generally characterized as attenuating excitability via V_{rest} hyperpolarization, APD shortening and decrease of AP amplitude. The effects of monounsaturated OEA appeared to be more pronounced and generally more consistent than those of saturated SEA, which agrees with previous findings that membrane ion channel-specific activity of NAEs correlates with the degree of their polyunsaturation [17–19].

Decrease of the amplitude and initial rate of rise of the AP by both NAEs indicated that they inhibit fast voltage-activated sodium current, I_{Na}, which is the major depolarizing current during the upstroke (phase 0) of the AP. Although this is the first direct demonstration of inhibitory action of NAEs on cardiac VGSCs, indirect evidence on such effects has been previously reported for neuroblastoma cells, in which 0.5 to 5 μM NAEs with carbon chain lengths of 14, 16 and 18 have been shown to inhibit the function of VGSCs measured by veratridine-activated Rb^+ efflux [20]. Furthermore, in rat hippocampal neurons the inhibition of action potential-evoked $[Ca^{2+}]_i$ increases by palmitoylethanolamide (3 μM) was attributed to its action on VGSCs since the compound failed to affect calcium influx associated with K^+-induced depolarization [21]. In cardiac

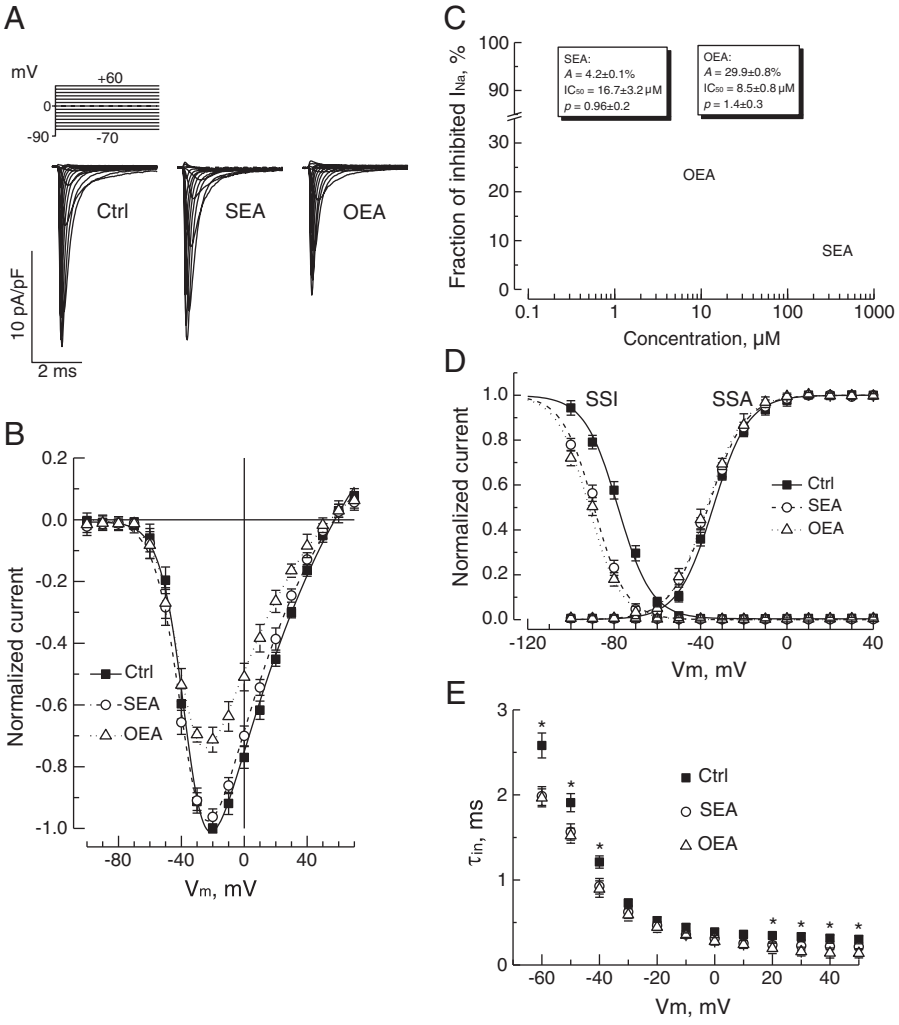

Fig. 5. Effects of SEA and OEA on voltage-activated sodium current (I_{Na}) in rat neonatal cultured cardiac myocytes. A: Representative recordings of I_{Na} in response to the depicted pulse protocol under control conditions (Ctrl) and after consecutive applications of 100 μM SEA and OEA. B: Normalized and averaged I–V relationships of control I_{Na} (filled squares, solid line) and I_{Na} in the presence of 100 μM SEA (open circles, dashed line) or OEA (open triangles, dotted line); symbols — experimental data points (mean ± s.e.m., from 5 myocytes), smooth lines — fit of experimental data points with the product of Boltzmann and Goldman–Hodgkin–Katz equation. C: Concentration–response relationships for the inhibitory action of SEA (open circles) and OEA (open triangles) on I_{Na}; symbols — experimental data points (mean ± s.e.m., from 4 to 7 myocytes), smooth lines — fit of experimental data points with Hill equation; parameters of the fits (maximal inhibition at saturating concentration, *A*, apparent half-maximal inhibitory concentration, IC_{50}, and cooperativity (Hill) coefficient, *p*) are shown in the plot. D: Steady-state activation (SSA) and steady-state inactivation (SSI) dependencies of control I_{Na} (filled squares, solid lines) and I_{Na} in the presence of 100 μM SEA (open circles, dashed line) or OEA (open triangles, dotted line); symbols — experimental data points (mean ± s.e.m., from 5 myocytes), smooth lines — fit of experimental data points with Boltzmann equation (see text for parameters). E: Voltage-dependence of I_{Na} inactivation time constant (τ_i) under control conditions (filled squares) and in the presence of 100 μM SEA (open circles) or OEA (open triangles); symbols — experimental data points (mean ± s.e.m., from 5 myocytes).

tissue, VGSCs are almost exclusively represented by their TTX-resistant $Na_v1.5$ isoform (gene *SCN5A*). Therefore, the changes in the biophysical properties of I_{Na} under the action of NAEs, namely induction of the hyperpolarizing shift in the voltage-dependence of its steady-state inactivation (SSI) can be attributed to their effects on $Na_v1.5$ channel gating.

A hyperpolarizing shift of the SSI indicates that a higher proportion of VGSCs would be inactivated at resting membrane potential and therefore substantially fewer channels would be available for activation, resulting in the decreased amplitude and rate of rise during the upstroke of the AP. OEA, in addition to its influence on VGSC inactivation, is likely to exert partial blockade of the channel's ion permeation since the hyperpolarizing shift of the SSI induced by OEA is only slightly higher than SEA, but at the same time OEA produces significantly stronger inhibition of I_{Na} (i.e., 30% vs. 4%, see Figs. 4B and 5B).

OEA was also found to be potent inhibitor of calcium current, I_{Ca}, which in cardiac tissue is mediated by $Ca_v1.2$ (gene *CACNA1C*) isoform of L-type VGCCs [22]. This current contributes to the plateau of the cardiac AP (phase 2), therefore, its suppression may be responsible for both the decrease of the amplitude of the plateau as well as shortening of the AP duration induced by NAE application. Our results show that OEA affects activation and inactivation gating of cardiac L-type VGCCs sufficient to produce a sizable reduction of I_{Ca} "window current" in the range of $V_m = -40$ mV to +10 mV, and induces partial blockade of the ion-conducting pathway leading to decreased amplitude of voltage-activated I_{Ca}.

Diminished stationary Ca^{2+} entry as a consequence of smaller "window current" may in part explain OEA-evoked enhancement of cardiomyocytes' viability via prevention of Ca^{2+} overload and reduction of necrosis, whereas inhibition of voltage-activated I_{Ca} may largely determine the decrease of the AP plateau amplitude and AP shortening observed in the presence of OEA. Overall, OEA-mediated suppression of voltage-activated I_{Ca} would provide clear negative inotropic effect, as evidenced by sizable attenuation of $[Ca^{2+}]_i$ transients and twitching magnitude in spontaneously beating myocytes. Although, to our knowledge, this is the first demonstration of the effects of NAE on the L-type VGCC of the cardiac muscle, similar results demonstrating the effects NAEs with various fatty acid chain lengths on skeletal muscle L-type VGCCs have also been described in biochemical studies [18,23].

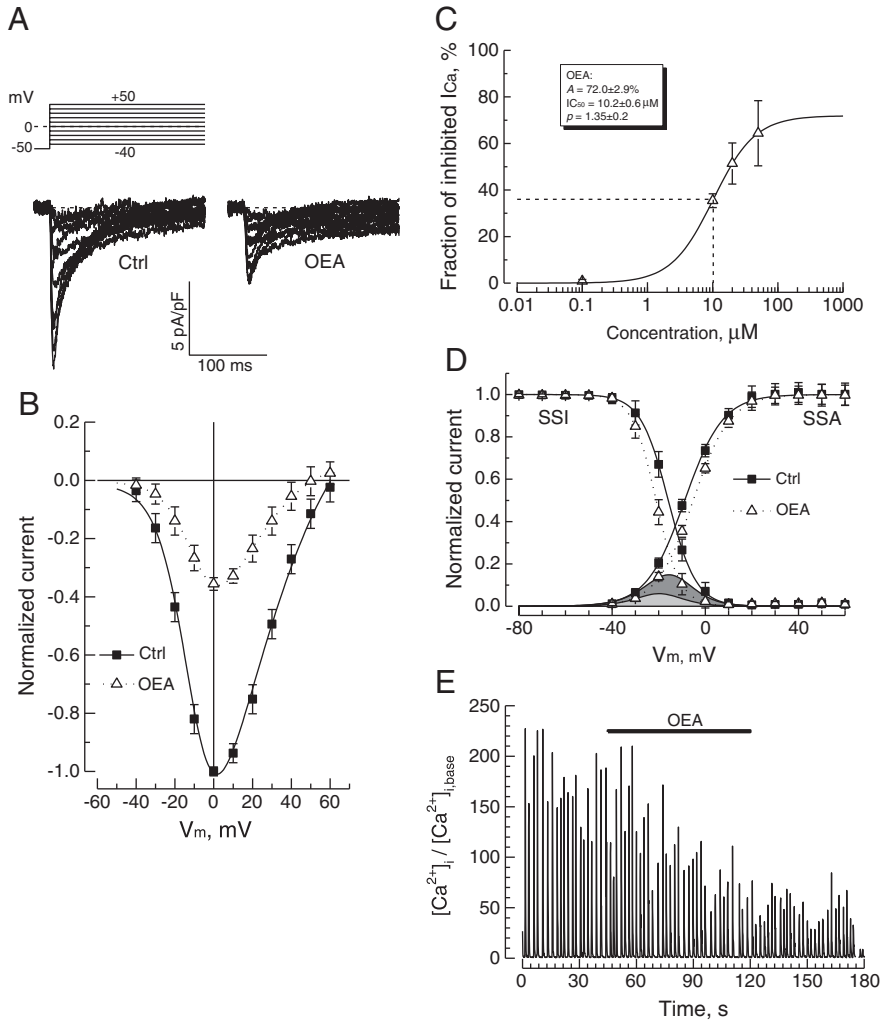

Fig. 6. Effects of OEA on voltage-activated calcium current (I_{Ca}) in rat neonatal cultured cardiac myocytes. A: Representative recordings of I_{Ca} in response to the depicted pulse protocol under control conditions (Ctrl) and after applications of 100 μM OEA. B: Normalized and averaged I–V relationships of control I_{Ca} (filled squares, solid line) and I_{Ca} in the presence 100 μM OEA (open triangles, dotted line); symbols — experimental data points (mean ± s.e.m., from 6 myocytes), smooth lines — fit of experimental data points with the product of Boltzmann and Goldman–Hodgkin–Katz equation. C: Concentration–response relationship for the inhibitory action of OEA (open triangles) on I_{Ca}; symbols — experimental data points (mean ± s.e.m., from 4 to 7 myocytes), smooth line — fit of experimental data points with Hill equation; parameters of the fits (maximal inhibition at saturating concentration, *A*, apparent half-maximal inhibitory concentration, IC_{50}, and cooperativity (Hill) coefficient, *p*) are shown in the plot. D: Steady-state activation (SSA) and steady-state inactivation (SSI) dependencies of control I_{Ca} (filled squares, solid lines) and I_{Ca} under the action of 100 μM OEA (open triangles, dotted line); symbols — experimental data points (mean ± s.e.m., from 6 myocytes), smooth lines — fit of experimental data points with Boltzmann equation (see text for parameters). E: Representative recordings of the $[Ca^{2+}]_i$ transients from spontaneously beating Fluo-4AM-loaded cardiomyocyte during application of 20 μM OEA (marked by horizontal bar).

Concerted actions of various K^+ and Cl^- channels determine the parameters of resting and action potentials of the cardiac muscle. Background activities of K^+ and Cl^- channels are known to be modulated by various extracellular ligands, intracellular second messengers or physicochemical factors including osmolarity, membrane tension, and pH [15,16]. Our findings indicate that SEA and OEA influence background conductance in a quite divergent manner, which probably reflects specific cardiac myocyte type-dependent expression of various K^+ and Cl^- channels as well as differential sensitivity of these channels to the NAEs investigated in this study. The disparity of SEA and OEA action on K^+ and Cl^- channels together with their inhibitory effects on VGSCs and L-type VGCCs might explain the wide range of changes of V_{rest} and AP parameters detected in our experiments. In the case of OEA we were able to separate three groups of myocytes in which the background conductance was decreased, unaltered or increased in the presence of OEA. It may well be that these groups represent three major types of myocytes, endocardial, epicardial and atrial, although more studies are needed to provide such correlation.

The increase of the background current in response to OEA occurred due to enhancement of its K^+ component, suggesting that OEA may up-regulate cardiac-specific inwardly-rectifying (i.e., I_{K1}, K_{ATP}, K_{ACh}) and/or 2P-domain (i.e., TASK-1, TREK-1, TWIK-1) K^+-channels that contribute to this component [17,24,25]. Further studies are needed to determine the targets of SEA and OEA among the cardiac K^+ and Cl^- channels.

In general, saturated and monounsaturated NAEs, which usually accounts for the majority of NAEs in most cells, are known to be cannabinoid receptor-inactive [4,26,27]. Thus, it is unlikely that direct activation of cannabinoid receptors mediates the effects of NAEs observed in this study. However, it has been suggested that some non-cannabinoid NAEs can serve as "entourage" compounds, which enhance the levels of cannabinoid receptor ligands, such as AEA and 2-arachidonylglycerol, thereby causing indirect activation of cannabinoid and/or vanilloid receptors [28–30]. Our control experiments with CB1 and TRPV1 receptor antagonists, AM251 (1 μM) and capsazepine (1 μM), respectively, failed to detect their influence on the inhibition of VGCC by SEA and OEA (data not shown), ruling out not only the involvement of these receptors, but also any potential entourage effect of studied NAEs on VGCCs. Thus, the action of SEA and OEA on cardiac VGSCs, VGCCs and background channels described in this study can be most likely explained by their direct interaction with the channels and/or by the modification of lipid

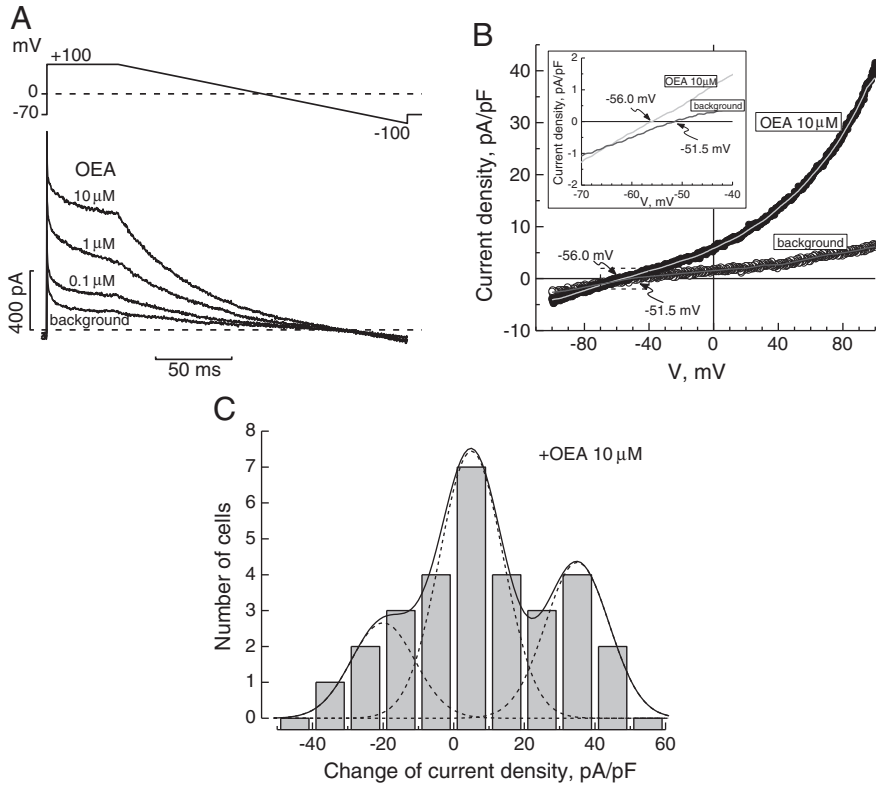

Fig. 7. Effects of OEA on background current in rat neonatal cultured cardiac myocytes. A: Representative recordings of the background current in response to the pulse protocol containing voltage ramp (shown above) in the myocyte, in which increasing concentrations of OEA caused progressive current enhancement. B: I–V relationships of the background current in the same myocyte derived from the ramp portions of the current recordings in the absence and in the presence of 10 μM OAE; inset is the expanded view of the I–Vs at intersection with voltage axis to demonstrate the values of the currents' reversal potential. C: Distribution of myocytes (columns) depending on the effect that 10 μM OAE produced on their background current (measured at +100 mV); solid line is the fit of the distribution with three Gaussians (dashed lines).

bilayer environment which is capable of influencing channel function, although further studies are needed to exclude possible involvement of other cannabinoid receptors such as GPR55 and GPR199 [31,32].

Endocannabinoid AEA in addition to CB receptor-mediated actions has been shown to modulate directly the activities of various VGSCs, VGCCs, and background K^+ channels in different cell types (for a review see [33]). Saturated SEA (18:0 NAE) and monounsaturated OEA (18:1 NAE), are structurally related to AEA (20:4 NAE), and several earlier studies have demonstrated that they also can have direct effects on the functions of various receptors such as TRPV1 [34,35], peroxisome proliferator-activated receptor alpha [36,37], ion channels such as VGCC [18,19,23], VGSC [20,21], and voltage-gated K^+ channels [38]. In agreement with our findings which showed higher potency of OEA compared to SEA, the extent of CB receptor-independent effects of NAEs on ion channels is generally determined by the degree of their unsaturation [17–19].

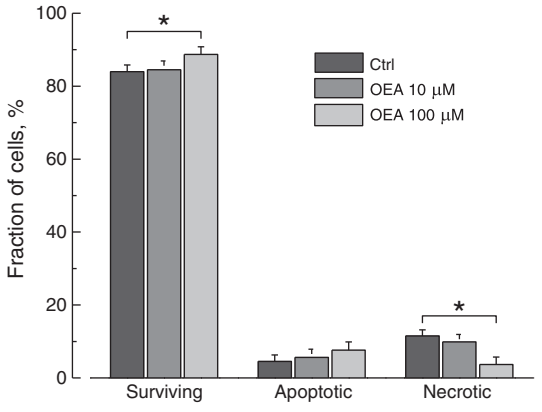

Fig. 8. Effects of OEA on viability of rat neonatal cultured cardiomyocytes. Bar graph (mean ± s.e.m. from 10 myocytes from 3 different cell cultures) showing general myocyte' survival and the split of overall myocytes' death on fractions resulting from apoptosis and from necrosis under control conditions (dark grey) and in the presence of 10 μM (grey) or 100 μM (light grey) OEA.

Considering their highly lipophilic structure, SEA and OEA can easily partition into the biological membranes and cause alterations of the lipid environment, which include hydrophobic mismatch between lipids and proteins, changes in membrane viscosity and in the interfacial curvature, altered lateral pressure profile, and shifts in lipid dipole potential and surface potential which can in turn affect the function of transmembrane proteins [33,39,40]. Specifically, it was proposed that lipophilic molecules such as AEA alter the free energy barrier required for conformational changes during the channel gating process [33,40]. In fact, not only SEA and OEA, but their corresponding free fatty acids such as stearic and oleic acids also modulate the functional properties of various ion channels and receptors [33].

In contrast to the classical hormones and neurotransmitters, NAEs are not stored in the intracellular compartments and released via exocytosis, but are synthesized and immediately liberated "on demand" via still poorly understood mechanisms. Increases of intracellular Ca^{2+} in response to cell depolarization or stimulation of G protein-coupled receptors (GPCRs) induce synthesis of numerous NAEs with a strong prevalence of those with saturated or weakly unsaturated long fatty acid chains, like SEA and OEA [3,41]. The amounts of released NAEs can drastically increase from normal physiological pico- or nanomolar concentrations to high micromolar concentrations under certain pathologies, especially during tissue ischemia [2,6,7,42,43]. Our results indicate that in cardiac myocytes, NAEs shown to be released during ischemic conditions can play cardioprotective role, as they lead to the attenuation of

electrical activity, decrease of Ca^{2+} entry, prevention of Ca^{2+} overload and enhanced resistance to necrosis.

Acknowledgements

This research was funded by the National Academy of Sciences of Ukraine and F46.2/001 grant from the State Fund for Fundamental Research, Ukraine.

References

[1] H.H. Schmid, P.C. Schmid, V. Natarajan, The N-acylation-phosphodiesterase pathway and cell signalling, Chem. Phys. Lipids 80 (1996) 133–142.
[2] H.S. Hansen, B. Moesgaard, H.H. Hansen, G. Petersen, N-Acylethanolamines and precursor phospholipids — relation to cell injury, Chem. Phys. Lipids 108 (2000) 135–150.
[3] N. Ueda, K. Tsuboi, T. Uyama, Enzymological studies on the biosynthesis of N-acylethanolamines, Biochim. Biophys. Acta 1801 (2010) 1274–1285.
[4] M. Maccarrone, A. Finazzi-Agrò, Endocannabinoids and their actions, Vitam. Horm. 65 (2002) 225–255.
[5] V. Di Marzo, Endocannabinoids, synthesis and degradation, Rev. Physiol. Biochem. Pharmacol. 160 (2008) 1–24.
[6] D.E. Epps, P.C. Schmid, V. Natarajan, H.H. Schmid, N-Acylethanolamine accumulation in infarcted myocardium, Biochem. Biophys. Res. Commun. 90 (1979) 628–633.
[7] N.R. Bachur, K. Masek, K.L. Melmon, S. Udenfriend, Fatty acid amides of ethanolamine in mammalian tissues, J. Biol. Chem. 240 (1965) 1019–1024.
[8] D.E. Epps, V. Natarajan, P.C. Schmid, H.O. Schmid, Accumulation of N-acylethanolamine glycerophospholipids in infarcted myocardium, Biochim. Biophys. Acta 618 (1980) 420–430.
[9] D. Marsh, M.J. Swamy, Derivatised lipids in membranes. Physico-chemical aspects of N-biotinyl phosphatidylethanolamines, N-acylphosphatidylethanolamines and N-acylethanolamines, Chem. Phys. Lipids 105 (2000) 43–69.
[10] O.I. Voitychuk, V.S. Asmolkova, N.M. Hula, H.V. Sotkis, M. Oz, Ia.M. Shuba, Regulation of the excitability of neonatal cardiomyocytes by N-stearoyl- and N-oleoyl-ethanolamines, Fiziol. Zh. 55 (2009) 55–66 (Ukrainian).
[11] O.I. Voitychuk, V.S. Asmolkova, N.M. Hula, M. Oz, Ia.M. Shuba, Effects of N-stearoyl- and N-oleoylethanolamine on cardiac voltage-dependent sodium channels, Fiziol. Zh. 56 (2010) 13–22 (Ukrainian).
[12] T.B. Rogers, S.T. Gaa, I.S. Allen, Identification and characterization of functional angiotensin II receptors on cultured heart myocytes, J. Pharmacol. Exp. Ther. 236 (1986) 438–444.
[13] R.D. Harvey, J.A. Jurevicius, J.R. Hume, Intracellular Na^{+} modulates the cAMP-dependent regulation of ion channels in the heart, Proc. Natl. Acad. Sci. U. S. A. 88 (1991) 6946–6950.
[14] S. Movafagh, L. Cleemann, M. Morad, Regulation of cardiac Ca^{2+} channel by extracellular Na^{+}, Cell Calcium 49 (2011) 162–173.
[15] J. Tamargo, R. Caballero, R. Gómez, C. Valenzuela, E. Delpón, Pharmacology of cardiac potassium channels, Cardiovasc. Res. 62 (2004) 9–33.
[16] D. Duan, Phenomics of cardiac chloride channels: the systematic study of chloride channel function in the heart, J. Physiol. 587 (2009) 2163–2177.
[17] M. Oz, Y. Tchugunova, M. Dinc, Differential effects of endocannabinoids and synthetic cannabinoids on voltage-dependent calcium fluxes in rabbit T-tubule membranes: comparison with fatty acids, Eur. J. Pharmacol. 502 (2004) 47–58.
[18] M. Oz, A. Alptekin, Y. Tchugunova, M. Dinc, Effects of saturated long-chain N-acylethanolamines on voltage-dependent calcium fluxes in rabbit T-tubule membranes, Arch. Biochem. Biophys. 434 (2005) 344–351.
[19] J. Chemin, J. Nargeot, P. Lory, Chemical determinants involved in anandamide-induced inhibition of T-type calcium channels, J. Biol. Chem. 282 (2007) 2314–2323.
[20] N.M. Gulaya, A.A. Melnik, D.I. Balkov, G.L. Volkov, M.V. Vysotskiy, V.E. Vaskovsky, The effect of long-chain N-acylethanolamines on some membrane-associated functions of neuroblastoma C1300 N18 cells, Biochim. Biophys. Acta 1152 (1993) 280–288.
[21] B.G. Kelley, S.A. Thayer, Anandamide transport inhibitor AM404 and structurally related compounds inhibit synaptic transmission between rat hippocampal neurons in culture independent of cannabinoid CB1 receptors, Eur. J. Pharmacol. 496 (2004) 33–39.
[22] W.A. Catterall, E. Perez-Reyes, T.P. Snutch, J. Striessnig, International Union of Pharmacology. XLVIII. Nomenclature and structure-function relationships of voltage-gated calcium channels, Pharmacol. Rev. 57 (2005) 411–425.
[23] A. Alptekin, S. Galadari, Y. Shuba, G. Petroianu, M. Oz, The effects of anandamide transport inhibitor AM404 on voltage-dependent calcium channels, Eur. J. Pharmacol. 634 (2010) 10–15.
[24] Y. Kubo, J.P. Adelman, D.E. Clapham, L.Y. Jan, A. Karschin, Y. Kurachi, M. Lazdunski, C.G. Nichols, S. Seino, C.A. Vandenberg, International Union of Pharmacology. LIV. Nomenclature and molecular relationships of inwardly rectifying potassium channels, Pharmacol. Rev. 57 (2005) 509–526.
[25] A. Gurney, B. Manoury, Two-pore potassium channels in the cardiovascular system, Eur. Biophys. J. 38 (2009) 305–318.
[26] H.H. Schmid, E.V. Berdyshev, Cannabinoid receptor-inactive N-acylethanolamines and other fatty acid amides: metabolism and function, Prostaglandins Leukot. Essent. Fatty Acids 66 (2002) 363–376.
[27] H.H. Schmid, P.C. Schmid, E.V. Berdyshev, Cell signaling by endocannabinoids and their congeners: questions of selectivity and other challenges, Chem. Phys. Lipids 121 (2002) 111–134.
[28] L. De Petrocellis, J.B. Davis, V. Di Marzo, Palmitoylethanolamide enhances anandamide stimulation of human vanilloid VR1 receptors, FEBS Lett. 506 (2001) 253–256.
[29] K.O. Jonsson, S. Vandevoorde, D.M. Lambert, G. Tiger, C.J. Fowler, Effects of homologues and analogues of palmitoylethanolamide upon the inactivation of the endocannabinoid anandamide, Br. J. Pharmacol. 133 (2001) 1263–1275.
[30] D. Smart, K.O. Jonsson, S. Vandevoorde, D.M. Lambert, C.J. Fowler, 'Entourage' effects of N-acyl ethanolamines at human vanilloid receptors. Comparison of effects upon anandamide-induced vanilloid receptor activation and upon anandamide metabolism, Br. J. Pharmacol. 136 (2001) 452–458.
[31] G. Godlewski, L. Offertáler, J.A. Wagner, G. Kunos, Receptors for acylethanolamides—GPR55 and GPR119, Prostaglandins Other Lipid Mediat. 89 (2009) 105–111.
[32] R.G. Pertwee, A.C. Howlett, M.E. Abood, S.P. Alexander, V. Di Marzo, M.R. Elphick, P.J. Greasley, H.S. Hansen, G. Kunos, K. Mackie, R. Mechoulam, R.A. Ross, International Union of Basic and Clinical Pharmacology. LXXIX. Cannabinoid receptors and their ligands: beyond CB1 and CB2, Pharmacol. Rev. 62 (2010) 528–531.
[33] M. Oz, Receptor-independent actions of cannabinoids on cell membranes: focus on endocannabinoids, Pharmacol. Ther. 111 (2006) 114–144.
[34] P. Movahed, B.A. Jönsson, B. Birnir, J.A. Wingstrand, T.D. Jørgensen, A. Ermund, O. Sterner, P.M. Zygmunt, E.D. Högestätt, Endogenous unsaturated C18 N-acylethanolamines are vanilloid receptor (TRPV1) agonists, J. Biol. Chem. 280 (2005) 38496–38504.
[35] V. Di Marzo, L. De Petrocellis, Endocannabinoids as regulators of transient receptor potential (TRP) channels: a further opportunity to develop new endocannabinoid-based therapeutic drugs, Curr. Med. Chem. 17 (2010) 1430–1449.
[36] H.S. Hansen, A. Artmann, Endocannabinoids and nutrition, J. Neuroendocrinol. 20 (Suppl. 1) (2008) 94–99.
[37] A.A. Izzo, F. Piscitelli, R. Capasso, P. Marini, L. Cristino, S. Petrosino, V. Di Marzo, Basal and fasting/refeeding-regulated tissue levels of endogenous PPAR-alpha ligands in Zucker rats, Obesity 18 (2010) 55–62.
[38] A. Barana, I. Amorós, R. Caballero, R. Gómez, L. Osuna, M.P. Lillo, C. Blázquez, M. Guzmán, E. Delpón, J. Tamargo, Endocannabinoids and cannabinoid analogues block cardiac hKv1.5 channels in a cannabinoid receptor-independent manner, Cardiovasc. Res. 85 (2010) 56–67.
[39] J.A. Lundbaek, P. Birn, A.J. Hansen, R. Søgaard, C. Nielsen, J. Girshman, M.J. Bruno, S.E. Tape, J. Egebjerg, D.V. Greathouse, G.L. Mattice, R.E. Koeppe, O.S. Andersen, Regulation of sodium channel function by bilayer elasticity: the importance of hydrophobic coupling. Effects of Micelle-forming amphiphiles and cholesterol, J. Gen. Physiol. 123 (2004) 599–621.
[40] C.E. Spivak, C.R. Lupica, M. Oz, The endocannabinoid anandamide inhibits the function of alpha4beta2 nicotinic acetylcholine receptors, Mol. Pharmacol. 72 (2007) 1024–1032.
[41] Y. Hashimotodani, T. Ohno-Shosaku, M. Kano, Ca^{2+}-assisted receptor-driven endocannabinoid release: mechanisms that associate presynaptic and postsynaptic activities, Curr. Opin. Neurobiol. 17 (2007) 360–365.
[42] H.S. Hansen, B. Moesgaard, G. Petersen, H.H. Hansen, Putative neuroprotective actions of N-acyl-ethanolamines, Pharmacol. Ther. 95 (2002) 119–126.
[43] C. Berger, P.C. Schmid, W.R. Schabitz, M. Wolf, S. Schwab, H.H. Schmid, Massive accumulation of N-acylethanolamines after stroke. Cell signalling in acute cerebral ischemia? J. Neurochem. 88 (2004) 1159–1167.